Dynamical Reconfigurable Master–Slave Control Architecture (DRMSCA) for Voltage Regulation in Islanded Microgrids

Wen Huang, *Member, IEEE*, Zhikang Shuai, *Senior Member, IEEE*, Xia Shen, Yifeng Li, and Z. John Shen, *Fellow, IEEE*

***Abstract*—Voltage fluctuation suppression and reactive power proportional sharing in islanded microgrids (MGs) are often difficult to maintain simultaneously. Hence, a dynamical reconfigurable master–slave control architecture is proposed herein. When a load fluctuates, the leader will be dynamically selected through specific features (such as the output power, output voltage, and power capacity); subsequently, the leader sends his information to all other distributed generators (DGs) as a unified signal in the MG. Meanwhile, the other DGs adjust their local output based on the unified reference to achieve accurate power sharing in each DG. Moreover, system voltage recovery can be realized simultaneously since each DG contains closed-loop voltage control. In addition, for the automatic selection of the leader, a dynamically selected method based on a weight-voting-based differential delay method is proposed herein; the method realizes the unicity and automatic selection of the leader during communication failure. Additionally, the stability of the proposed method is proven mathematically. The results show that the proposed method is stable for any communication period and DG quantity. Furthermore, the communication delay and communication failure are derived mathematically. The results show that the proposed method demonstrates robustness against communication delay. Finally, experimental results verify the effectiveness of the proposed method under communication delays, failures, and power failures.**

***Index Terms*—Dynamical reconfigurable master–slave control, islanded microgrid (MG), reactive power sharing, voltage regulation.**

I. Introduction

MICROGRIDS (MGs) are important for the rational utilization of renewable energy sources and coping with energy crises [1]–[6]. However, the reactive power distribution and bus voltage of MGs are significantly affected by the line impedance since MG structures are relatively small and the output of distributed generators (DGs) fluctuate frequently [7]. These factors render it difficult to achieve reactive power sharing and voltage fluctuation suppression in MGs simultaneously; hence, the long-term reliable operation of DGs and the safe power supply for power users are affected significantly [2], [8].

Currently, two main classes of voltage control methods for islanded MGs exist: strategies with and without communication. The targets of the two methods are exactly opposite. The control strategy without communication is typically more reliable because no communication is involved; as such, researchers often focus on the performance optimization. Meanwhile, for the control strategy with communication, because of the existence of communication, good performances can be guaranteed; nonetheless, the possible unreliability of communication has motivated researchers' toy focus on reliability improvement [9]. Schemes without communication primarily employ local information as much as possible and combine the network information to achieve voltage control [10]–[14], e.g., in droop control, virtual impedance control [2], [15], [16], and the virtual frame transformation method [17]. Although these methods alleviate the contradiction between voltage fluctuation suppression and reactive power sharing to some extent, their performances are sensitive to the line impedance and local parameters. A trade-off remains between voltage recovery and accurate reactive power sharing. In [18], a method for simultaneously realizing efficient power sharing and the point of common coupling (PCC) voltage control by introducing the PCC voltage into local controllers is proposed. Nevertheless, it is noteworthy that as the MG scale increases, the random distribution of line cables and loads will result in an ambiguous PCC voltage. Therefore, the method presented in [18] will not yield the desired control targets.

Meanwhile, schemes with communication to transmit the state information of DGs for solving the contradiction between voltage stability and reactive power sharing in islanded MGs have been proposed by many researchers. These schemes can be primarily categorized into two types. In the first type, an additional central controller or a specific DG is employed as the central control unit for obtaining/processing information regarding all DGs, and after sending a feedback command to ensure system voltage stability and power sharing [19]–[21].

Manuscript received December 29, 2020; revised April 20, 2021 and June 18, 2021; accepted July 17, 2021. Date of publication July 26, 2021; date of current version September 16, 2021. This work was supported in part by the National Natural Science Foundation of China under Grant 51977066, in part by the Science and Technology Innovation Program of Hunan Province under Grant 2020RC4015, and in part by the Hunan Provincial Innovation Foundation for Postgraduate under Grant CX20200433. Recommended for publication by Associate Editor Y. Xue. *(Corresponding author: Zhikang Shuai.)*

Wen Huang, Zhikang Shuai, and Xia Shen are with the College of Electrical and Information Engineering, Hunan University, Changsha 410082, China (e-mail: huangwen@hnu.edu.cn; szk@hnu.edu.cn; shenxia@hnu.edu.cn).

Yifeng Li is with the State Grid Corporation of China, Changsha 410004, China (e-mail: 717121203@qq.com).

Z. John Shen is with the Department of Electrical and Computer Engineering, Illinois Institute of Technology, Chicago, IL 60616 USA (e-mail: zjohnshen@gmail.com).

Color versions of one or more figures in this article are available at https://doi.org/10.1109/TPEL.2021.3099482.

Digital Object Identifier 10.1109/TPEL.2021.3099482

The advantage of this method is that the entire system comprises only one predefined leader. The system is more likely to remain stable if communication is not severely affected. However, its performance depends significantly on the central control unit. Once the central control unit fails, the MG will lose the ability to recover voltage; consequently, the reliability and redundancy will be insufficient. The second type is primarily based on the distributed consensus algorithm for achieving MG voltage fluctuation control [22]–[27]. The basic principle is to exchange information including those pertaining to the voltage and reactive power through communication between adjacent DGs, as well as achieve voltage fluctuation control and reactive power sharing through internal closed-loop control. In [22], a method for distributed secondary control using linear input–output feedback was proposed. In [23], voltage recovery and accurate reactive power sharing were realized by the proposed consensus algorithm. In [24], consensus control and local proportional integral (PI) compensation were combined to solve problems pertaining to voltage recovery and reactive power distributions under high R/X situations. Similarly, based on consensus control, the problem of reactive power sharing in an MG with an unknown topology was addressed in [25]. A two-layer optimal consensus-based distributed control strategy is proposed in [28]. In [29], a consensus-based distributed control for accurate reactive, harmonic, and imbalance power sharing is proposed. In [30], a hierarchical control scheme for accurate load sharing and power quality enhancement in networked MGs with unbalanced load currents is proposed. A distributed control imposing a time-varying droop gain and specifying the virtual voltage drop is proposed in [31]. However, this type of method typically exhibits the following shortcomings.

1) The average-consensus-based consensus algorithm has been widely used. However, information regarding all surrounding DGs must be acquired to obtain the average value. The reactive power and voltage information are required simultaneously, and the local communication bandwidth requirement is high.
2) The real-time requirements of communication are high [32]–[34]. When the communication period or communication delay is long, system response confusion and system instability will likely occur since all DGs are in fact independent leaders, and each can influence the others around it [32].

To address the issues above, we previously [33] proposed an maximum power loading factor (MPLF)-based secondary frequency regulation control method for island MGs; this method achieves effective frequency control and reasonable distribution of active power simultaneously. However, the method proposed in [33] is limited to frequency control and cannot solve the possible split-brain phenomenon due to communication line failure. Additionally, the authors of [33] failed to prove the system stability under an increasing system scale and by considering a longer communication period mathematically.

A dynamical reconfigurable master–slave control strategy with low-bandwidth communication based on a previous study is proposed herein [33]. In this strategy, only one leader exists at each time instance in the MG. This preserves the advantages of easy consistency realization in centralized control methods. More importantly, the leader can be selected automatically based on the MG status, thereby overcoming the leader failure problem in centralized control. The contributions of this article are as follows.

1) By fully utilizing the advantages of easy consistency realization of conventional centralized control schemes and combining them with the proposed automatic leader selection method, a dynamical reconfigurable master–slave control strategy is proposed. The strategy is suitable for MG voltage fluctuation control and can overcome the over-reliance upon a central controller in the conventional master–slave architecture.
2) A new leader selection method is proposed. Not only the maximum output information, but also other information such as output voltage, DG capacity, PCC voltage, and economic operation factors can be used as criteria for selecting the leader to achieve effective control and multiobjective optimization of critical loads or PCC voltages.
3) The differential delay method is improved, and the leader automation selection method based on the election voting principle is presented. When the communication line is broken into two subsystems owing to fault, only the subsystem with more votes can generate a new leader, whereas the subsystem with fewer votes will switch from secondary control to the droop control operation.
4) The stability of the proposed method under an infinite system scale and communication period is proven, and the conservative range of communication delay is deduced to ensure the stability of the system, thereby providing a theoretical foundation for the practical application of the proposed method.

The remainder of this article is organized as follows. The basic principle of the proposed dynamical reconfigurable master–slave control strategy for voltage regulation in islanded MGs as well as the differential delay and weight voting methods (DDWVM) are discussed in Section II. The tolerance of the DG quantity as well as the long communication period and delay of the dynamical reconfigurable master–slave control architecture (DRMSCA) are theoretically analyzed in Section III. Experimental verifications are presented in Section IV. Finally, the conclusion is summarized in Section V.

II. Dynamical Reconfigurable Master–Slave Control Architecture

The basic structure of an islanded MG with communication is shown in Fig. 1. A communication bus is applied to exchange information among the DGs. As a grid-friendly interface, a virtual synchronous generator (VSG), which is an improved droop control that can realize medium–high frequency fluctuation suppression of MGs, was utilized [35], [36]. Therefore, the VSG was the main control in the distributed energy resources (DERs) of islanded MG in this article.

A. Principle of Proposed DRMSCA

The primary regulation of the traditional islanded MG voltage can be automatically achieved by relying on the drooping

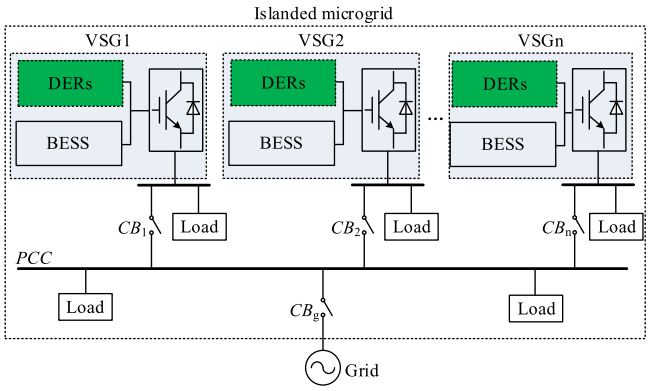

Fig. 1. Islanded microgrid structure with communication.

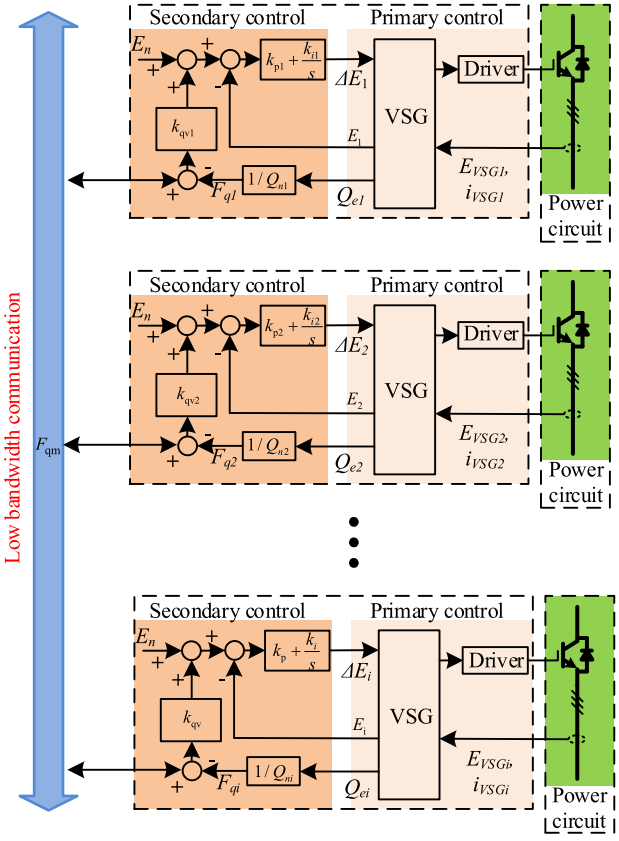

Fig. 2. Scheme of proposed DRMSCA with low-bandwidth communication.

characteristics of the VSG. To further reduce the steady-state error of the MG voltage during power fluctuations, an islanded MG voltage control method based on the dynamic reconfigurable master–slave structure is proposed herein. The basic principle is shown in Fig. 2.

In Fig. 2, $i_{\mathrm{VSG}i}$ is the inverter output current; ΔE_i is the compensation amount specified by the VSG voltage; E_n is the inverter reference voltage; E_{i} is the port voltage of the ith VSG; F_{qi} is the local output factor; F_{qm} is the output factor of the system leader; Q_i is the reactive output of the local inverter; Q_{ni} is the rated reactive power of the local inverter; k_{qv} is the proportional coefficient; k_p and k_i are the proportional and integral coefficients, respectively.

As shown in Fig. 2, the DRMSCA voltage control method proposed herein is primarily composed of three components, i.e., the communication module, a distributed VSG secondary control module, and the primary control module. The communication module enables information exchange among the DERs; the secondary control receives the reference signal transmitted by the communication module to realize the secondary regulation of the local DG voltage and the proportional sharing of the system power; the primary control module primarily realizes the primary voltage regulation of the MG.

The core idea is to achieve the parallel movement of the droop characteristic curve by adjusting the reference voltage of the primary control such that proportional power sharing and effective voltage control can be achieved.

In a specific time period, the entire system comprises only one leader. The leader coordinates the output of the entire system by sending its own output information, and the main function of the leader is to realize voltage recovery such that the average system power distribution and system voltage recovery can be realized simultaneously. Furthermore, the leader uses the differential delay weight voting method to ensure that the unit with voting rights in the system can become a leader; in this case, when one of the systems or the leader errs, the second candidate unit becomes the new leader immediately and continues to lead the normal operation of the system. The differential delay weight voting method will be discussed in detail in the next section.

It should be noted that accurate reactive power sharing and zero-error voltage regulation cannot be satisfied at the same time indeed, especially when considering the influence of line impedance. The proposed method is dedicated to minimizing the reactive power sharing error while keeping the system voltage close to the rated voltage.

To achieve the secondary regulation of the voltage and the proportional sharing of the reactive power by reducing the communication complexity as much as possible, an output factor is proposed herein. It is used as the reference information of the system reference unit to the communication bus, and its formula is shown in

$$F_q = \frac{Q_e}{Q_n}. \tag{1}$$

In the formula, Q_e is the active power output of the inverter, and Q_n is the rated active power of the inverter. As shown in (1), the output factor comprises both the rated power and actual output power. When the output factors of the VSG units in the system remain the same, it signifies that the reactive output of the VSG has been achieved and is proportional to the rated capacity.

In addition, it is noteworthy that the addition of sharing approximates the magnitude of the output factor to the standard value, i.e., generally between 0 and 2, thereby significantly reducing the requirement for the data transmission bit width of the communication system. The bus is only required to transmit a signal with the maximum output factor, and this can significantly reduce the requirements of communication and realize low-bandwidth communication.

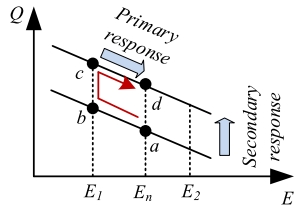

Fig. 3. Voltage regulation process of DRMSCA.

Fig. 2 illustrates the operating principle of the proposed method comprehensively:

$$F_{qm} = f\left(F_{q1}, F_{q2}, \ldots, F_{qn}\right) \tag{2}$$

$$E_{refi} = E_{\mathrm{n}} + k_{qv}(F_{\mathrm{qm}} - F_{qi}) \tag{3}$$

$$\Delta E_i = k_p(E_{refi} - E_i) + k_i \int (E_{refi} - E_i)dt \tag{4}$$

where F_{qm} is the output factor of the leader in the MG, $E_{\mathrm{ref}i}$ is the reference value of the voltage, and E_i is the actual port voltage of the ith inverter.

The Q–V dynamic characteristics of the proposed method are shown in Fig. 3. The primary control can be regarded as a lateral movement along the curve, whereas secondary regulation as a vertical translation of the curve. Assume that the system is operating at a point in the initial state. When the load power increases, the power balance of the system is broken, the system voltage is reduced gradually, and the operating point of the system moves from point a to b. At this time, in the secondary control module, the voltage control inner loop will quickly generate the regulation of the voltage based on the voltage differences of the system and then transmit it to the primary control module such that the system operation point moves from point b to c. Finally, under the primary control, the system work point shifts from point c to point d to achieve voltage recovery. In the entire regulation process, the main function of communication is to transmit the reference information to adjust the voltage of the non-F_{qm} DER to yield E_{ref}, adjust the power allocation of each VSG unit of the system, and finally realize the secondary regulation of the system voltage and the proportional sharing of the power.

After the system stabilizes, two situations are encountered.

When the system is finally stable and the communication is unobstructed, the output factor of the leader is the same as the local output factor. At this time, the output factor ratio of the outer loop is zero, and its control is degraded to the tracking of the local voltage to a specified voltage. Moreover, owing to the integral effect of internal loop compensation, the local voltage can always be maintained equal to the voltage of the system.

If a fault occurs in the system communication, then the system will select a leader, and the normal communication can still achieve the secondary regulation of the voltage, whereas the communication fault exits the secondary regulation and maintains the droop characteristic; for the part with a leader, the secondary regulation of the voltage can still be achieved to ensure that the system voltage is always stable within the required range.

In particular, the voltages in the system are not exactly equal due to the impedance of the line. Therefore, the proportional part of the secondary regulation part cannot completely eliminate the steady-state error; however, because of the zero-error tracking of the leader of the output voltage, the system voltage will still approach the rated value, thereby reducing the voltage fluctuation range.

B. Dynamical Leader Selection Method

In the previous section, the basic principles and implementation process of the proposed method were presented. However, in practical applications, the independent selection of the leader presents technical difficulties—particularly, the automatic seamless switching of the leader and the communication system splitting problem when the communication fails. To solve these problems, a differential delay weight voting method is proposed herein.

1) Basic Principle of Differential Delay Weight Voting Method: In this article, the CAN communication bus is used as the physical basis, and the communication interface of each VSG in the MG is uniformly adopted by the CAN bus protocol. According to the communication principle of the consistency algorithm, a differential delay weight voting method is proposed to realize the automatic selection of the leader.

The core of the method consists of two parts: the differential delay part and the weight voting part. The differential delay part can obtain the communication right and determine the length of delay times through the combination of local feature quantities. Moreover, the DG with shorter delay gives priority to the leader, considering the different delay times of the DGs in the MG. The weight voting part is used to prevent the whole system from splitting into two communication subsystems when the communication system is faulty. When the leader changes, the system initiates a vote, and the weight coefficient of different DGs is reflected in the difference in votes. When the unit receives more than half of the votes, it can become a new leader, ensuring that there is only one or zero leader in the entire system. The two core parts are studied further in the next section.

Fig. 4 presents a detailed flowchart of the proposed method, where F_q is the received output factor, F_{qi} is the local output factor, and F_{qm} is the selected leader output factor. t_D is defined as follows:

$$t_D = f(D_Q) \tag{5}$$

where t_D represents the differed delay time, and D_Q represents the output-factor difference between the local and the leader.

The workflow of the differential delay weight voting method is as follows.

When the system does not select the leader, each DG substitutes the current local feature information (such as output, frequency, voltage, and capacity) and calculates a local delay time according to the same rules. The delay time of the DG is different, and the unit with the shortest delay time may become the new leader. When the unit with the shortest delay reaches the delay time, it sends its current output factor to the communication bus. When the other DG receives the output

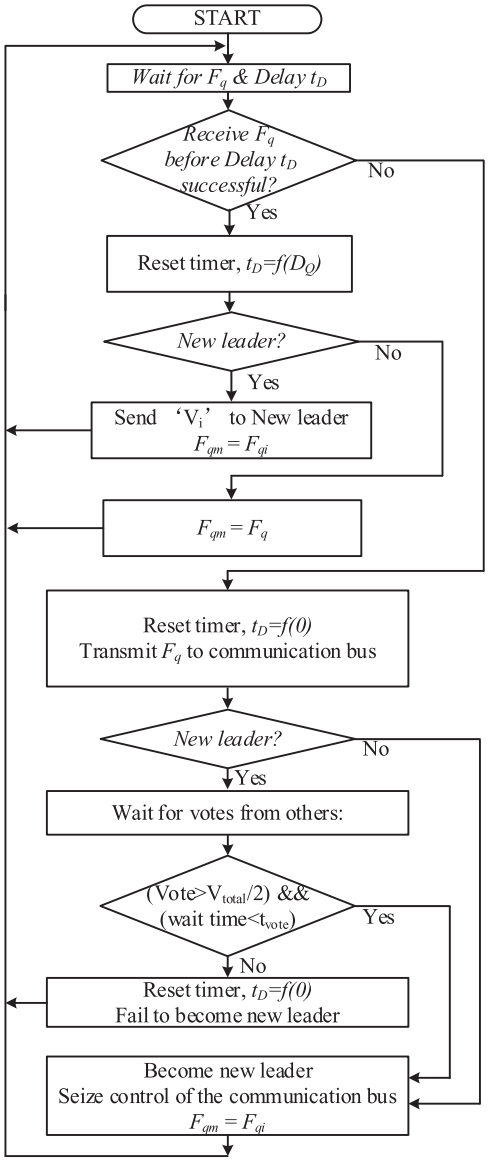

Fig. 4. Flowchart of the differential delay and the weight voting method.

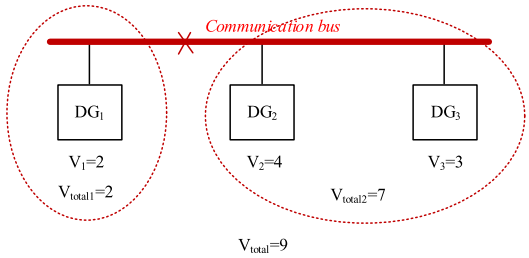

Fig. 5. Voting principle of the subsystem leader when communication fails.

factor sent by the unit for the first time, it sends the number of votes representing the weight information of this DG to the unit. Once the candidate of the leader receives more than half of the votes within the specified time, the unit officially becomes the new leader and sends its output information to other DGs again. When other DGs receive the output information of the same unit twice in a row, it can be considered that a new leader is selected, and the output information of the leader is used as a local reference to make the system output consistent.

When the leader receives less than half of the votes within the regular time, it withdraws from the election of the leader, and the second DG, which has the second-longest delay time, continues to participate in the election of the leader, and so on. If there is no fault in the system, the unit with the shortest delay time can always be selected as the only leader. While the communication failure occurs in the system, only the number of votes in the communication network reach more than half, the only leader can be selected. However, the other subcommunication networks with fewer votes are unable to select the leader and then exit the secondary regulation.

2) Principle of the Distribution of Votes of Different DGs: The workflow for the election voting process is as follows. When the candidate first reaches the delay time, it sends its own output factor as defined in (1) to the others, and the other units reset the local delay timer after receiving the information and issue approval votes to the candidate. The votes sent to the leader by others are continuously received within a set time after the information is sent. When the number of votes is greater than half in a set time, the change of the leader can be considered valid. Then, the unit becomes the new leader, and when no new leader takes over, no new election process is conducted. The unit sends only its own output information to other units to ensure system coordination.

Additionally, the unit is allowed to allocate a certain number of votes to different units in advance. For example, a larger capacity energy-storage station gains more votes. Thus, when the communication fails, it is beneficial to ensure that the secondary regulation of the portion with a large capacity maintains a normal state to the greatest extent possible

$$Vote = f(Q_{\mathrm{n}}). \tag{6}$$

In practice, the allocation of votes can consider various factors, such as the type of device, economy, and security. This is an open point, and more research can be conducted in practical applications. In this article, only the output power factor is considered as an example [33].

Each time a new leader is selected, the priority order is determined according to the delay information, and then the new candidate must obtain more than half of the votes to become the official leader.

In Fig. 5, V_i represents the number of votes assigned to the micro-source, $V_{\mathrm{total}\,i}$ represents the total number of votes of the subsystem ($i = 1, 2$); and V_{total} represents the total number of votes of the system.

When the communication fails, the communication system is decomposed into two subsystems. At this time, the total number of votes of the subsystems where DG_2 and DG_3 are located is 7, which is 4.5 votes more than half. It is possible to select a new leader, which will still maintain secondary voltage control. For the subsystem where DG_1 is located, because the number of votes is 2, the requirement of having more than half of the votes is not satisfied, and the new leader is not selected. Therefore,

because the unit cannot be selected as the leader in multiple elections, it withdraws from the secondary control later and returns to the droop control state. The total number of votes is set to an odd number for ensuring that the system does not have exactly the same number of votes for the two subsystems.

The choice of the delay function in the differential delay method is used to determine which unit has the priority to be the leader for ensuring that the critical load of the system or the voltage of the PCC bus is stable. The allocation of the number of votes is used to determine that if the system is split into two systems, one subsystem can become a secondary regulation system, and the other subsystem degenerates into droop control, avoiding the selection of two leaders and resulting in the safety of the system.

III. Stability Analysis of the Proposed DRMSCA

In this part, the system stability is verified in the case of the increased DG quantity and the communication influence. Hence, the tolerance and stability of the proposed method at the system scale are derived. Then, the communication delay is theoretically derived.

A brief introduction to the mathematical methods is presented in this part. The traditional consensus convergence judgment theory based on small-signal analysis is difficult to apply in cases of discontinuous intermittent communication and long delays systems [34], [37]. Thus, considering the characteristics of periodic communication, this article proposes a method to prove the stability of the system according to whether there is a convergence solution for the system steady-state equation. Because the power-adjustment process of the local primary control is far shorter than that of the secondary control, the following three assumptions are made for the convenience of analysis.

1) The system has reached a stable state before each communication occurs.
2) The load of the system is stable for a period of time after one or more fluctuations.

The state of the entire system at this time depends on the iterative process of the periodic communication under the initial conditions. Therefore, the stability of the proposed method can be analyzed by referring to the iterative convergence judgment condition in the numerical calculation, as indicated by

$$\lim_{n\to\infty} \mathbf{x}^{(n)} = \mathbf{x}^{*}. \tag{7}$$

Clearly, when n tends to infinity, if $\mathbf{x}*$ exists, the system converges. The following derivations are based on this mathematical foundation.

A. Effect of Communication Delay on Differential Delay Weight Voting Method

For the CAN bus protocol, only one device can occupy the communication bus at a time. Thus, when a VSG is sending data, the other VSGs are unable to perform this action, because the communication will fail owing to the data conflict. The operation process of the DDWVM with a communication delay is shown in Fig. 6 [33]. VSG_1 is assumed to be the leader in the previous cycle.

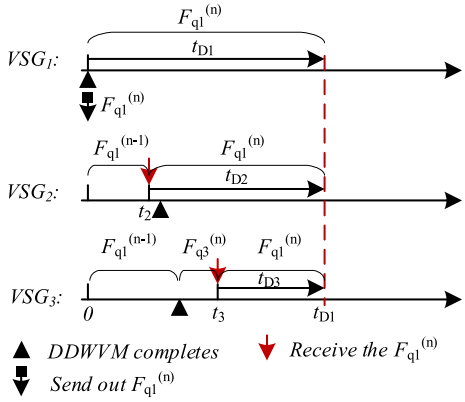

Fig. 6. Operation process of DDWVM in one cycle when there is communication delay.

In Fig. 6, $F_{\mathrm{q}}{}^{(n-1)}$ represents the output factor of the previous cycle; $F_q{}^{(n)}$ represents that of the current cycle; t_2 and t_3 represent the total communication delays from VSG_1 to VSG_2 and VSG_3, respectively (including the delays in the communication bus, equipment, and DSP controller); and t_{D1}, t_{D2}, and t_{D3} represent the differential delays, which are defined by (5), in the current cycle of three VSGs.

Assuming that VSG_1 is the leader in the previous cycle, it will be the first VSG to complete the differential delay according to (5). Then as shown in Fig. 6, it will occupy the communication bus to broadcast its own output factor, i.e., $F_{q1}{}^{(n)}$, at $t = 0$. The situations of VSG_2 and VSG_3 are analyzed in the following sections.

After VSG_1 completes the previous differential delay, it immediately occupies the communication bus and restarts the current differential delay (t_{D1}) before sending data to VSG_2 and VSG_3. During the period of t_{D1}, the controller forbids the data-sending request from VSG_2 and VSG_3 to the bus.

When VSG_2 receives the data successfully before the end of t_{D1}, VSG_2 first cancels the request to send itself data and sets F_q as the reference $F_{q\max}$. Then, the differential delay t_{D2} can be started. If VSG_2 wants to occupy the communication bus and become the system leader for the next period, the following must be satisfied:

$$\mathrm{t}_2 + t_{D2} < t_{D1}. \tag{8}$$

Similarly, after VSG_2 becomes the system leader, if VSG_1 wants to regain the communication right from VSG_2, (9) must be satisfied by assuming that the time-delays of data sending between VSG_1 and VSG_2 are equal

$$\mathrm{t}_2 + t_{D1} < t_{D2}. \tag{9}$$

Therefore, even when there is a communication delay, the current leader can effectively send signals to other VSGs. The main consequence is that VSGs with a longer communication delay have more difficulty obtaining the communication right than those with no delay, as indicated by (8). Nonetheless, once a VSG becomes the system leader, the foregoing situation will

be reversed, as indicated by (9). Thus, a certain communication delay grants the leader a hysteretic nature, which can prevent frequent changes of the leader and is beneficial to the system stability.

The foregoing analysis involves the situation where the leader does not change during one period, and there is no need to consider the delay effect of the voting process. When the leader changes and voting is needed, the main process is similar to that described above; however, the candidate who reaches the difference delay time first sends its own information to other VSGs. After other units receive the information and perceive the leader change, they send the votes that they hold to the new candidate when the CAN bus is idle. The communication delay here determines whether the candidate can receive sufficient votes within a limited time. If the communication delay is short and the candidate can receive sufficient votes, it will become the new leader. If the communication delay is too long, the candidate cannot receive sufficient votes for becoming the new leader, and the previous leader continues to play the leading role.

Generally, the CAN-bus-based DDWVM can ensure that the system only has one unified reference signal under the condition of communication delay, which can ensure the voltage regulation and reactive power-sharing characteristics.

B. Effects of DG Quantity and Communication Period on Stability of DRMSCA

When the system is stable, from the perspective of power balance, the following equations should hold (for the convenience of analysis, take the first unit as the leader, and the 2nd to *n*th units as the followers):

$$\begin{cases} E_{ref1}+k_1Q_1^{(n)}=(k_1+D_{p1}+\frac{X_1}{E_{ref1}})Q_1+U_{pcc} \\ E_{ref2}+k_2Q_1^{(n)}=(k_2+D_{p2}+\frac{X_2}{E_{\mathrm{ref2}}})Q_2+U_{pcc} \\ \vdots \\ E_{refn}+k_nQ_1^{(n)}=(k_n+D_{pn}+\frac{X_n}{E_{\mathrm{ref}n}})Q_n+U_{pcc} \\ \sum\limits_{i=1}^{n}Q_i=Q. \end{cases} \tag{10}$$

In (10), $E_{\mathrm{ref}i}$ represents the internal reference voltage of the *i*th inverter, k_i is the adjustment coefficient of the DRMSCA, Q_i represents the reactive power output of the *i*th inverter, X_i represents the reactance between the inverter port and the PCC, U_{pcc} represents the voltage at the PCC point, and Q represents the reactive load.

At the same voltage level, the internal voltage reference value of the DGs can be easily set to the same value, thus the following can be easily satisfied:

$$E_{\mathrm{ref1}}=E_{\mathrm{ref2}}=\cdots=E_{\mathrm{ref}n}. \tag{11}$$

Therefore, by introducing (10), (11) can be simplified and transformed into (12).

For (12) further deformation, substitute (12) into (10), (13) can be obtained. Then, (13) can be modified to obtain the iterative expression of (14).

According to (14), the output of the leader in each communication slice can be solved when the output of each DG reaches a stable state; then, using (10), the output of all DGs can be solved. Therefore, the system converges to a unique solution and is stable.

Obviously, the convergence condition of (14) can be obtained in (15).

The convergence region of the convergence condition must be judged according to the actual system information, which can be considered when designing the system parameters. Here, considering that the number of degrees of freedom k is larger than the droop coefficient D_p, there is no need to consider the local power characteristics in detail. Therefore, a conservative but simpler and more suitable sufficient condition of (15) can be obtained as (16).

Clearly, because k differs from the droop coefficient, it has little relationship with the local DG capacity. In actual applications, it can be set to a uniform value for the entire system, and the convergence expression is given by (17)

$$\sum_{i=1}^{n}\frac{1}{(k_i+D_{pi}+\frac{X_i}{E_{\mathrm{ref}}})}(E_{ref}-U_{\mathrm{pcc}}) +\sum_{i=1}^{n}\frac{k_i}{(k_i+D_{pi}+\frac{X_i}{E_{ref}})}Q_1^{(n)}=Q \tag{12}$$

$$\begin{aligned}&\sum_{i=1}^{n}\frac{1}{(k_i+D_{pi}+\frac{X_i}{E_{ref}})}(E_{ref}-U_{pcc}) \\ &=\sum_{i=1}^{n}\frac{1}{(k_i+D_{pi}+\frac{X_i}{E_{ref}})}\left(k_1+D_{p1}+\frac{X_1}{E_{ref}}\right)Q_1 \\ &\quad-\sum_{i=1}^{n}\frac{k_i}{(k_i+D_{pi}+\frac{X_i}{E_{ref}})}Q_1^{(n)}\end{aligned} \tag{13}$$

$$\begin{aligned}Q_1^{(n+1)}=&\frac{Q}{\sum\limits_{i=1}^{n}\frac{k_1+D_{p1}+\frac{X_1}{E_{ref}}}{k_i+D_{pi}+\frac{X_i}{E_{ref}}}} \\ &+\left(\frac{\sum\limits_{i=1}^{n}\frac{k_1}{(k_i+D_{pi}+\frac{X_i}{E_{ref}})}-\sum\limits_{i=1}^{n}\frac{k_i}{(k_i+D_{pi}+\frac{X_i}{E_{ref}})}}{\sum\limits_{i=1}^{n}\frac{k_1+D_{p1}+\frac{X_1}{E_{ref}}}{(k_i+D_{pi}+\frac{X_i}{E_{ref}})}}\right)Q_1^{(n)}.\end{aligned} \tag{14}$$

When (17) holds, the system remains stable. Additionally, it should be noted that the derivation and solution here do not involve the communication period or specify the DG quantity; thus, the convergence condition can always be satisfied in any long communication period with any DG quantity.

The following conclusions can be drawn through the mathematical derivation.

1) In the case of a constant load, the proposed DRMSCA is stable.
2) When the communication period is longer than the local response time, the proposed DRMSCA is stable for any communication period.

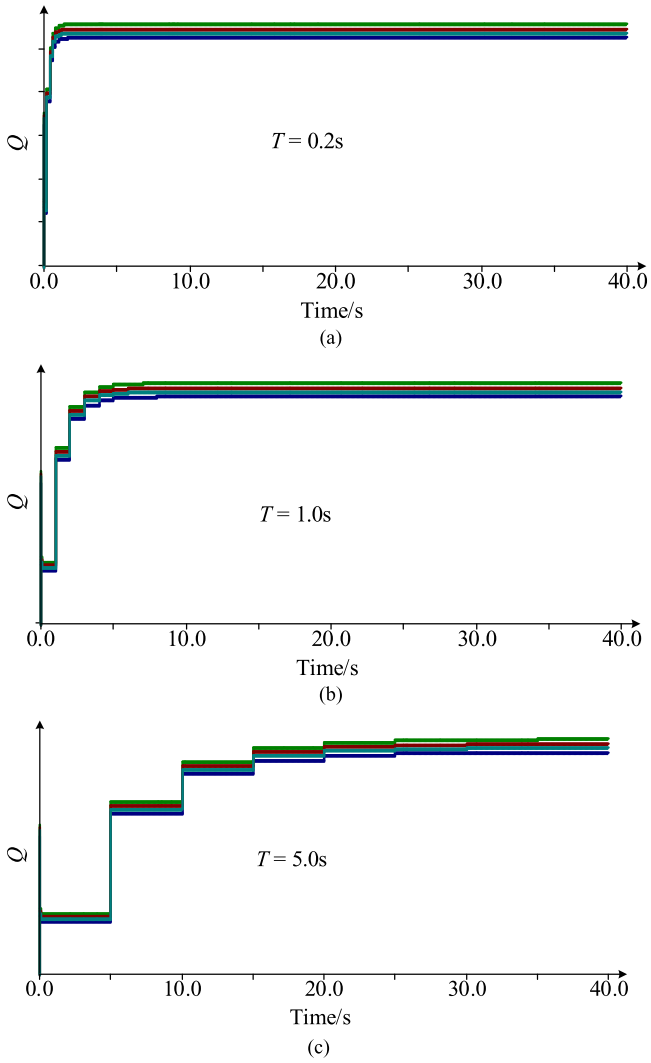

Fig. 7. Simulation results for the DRMSCA with different communication periods: (a) 0.2 s; (b) 1 s; (c) 5 s.

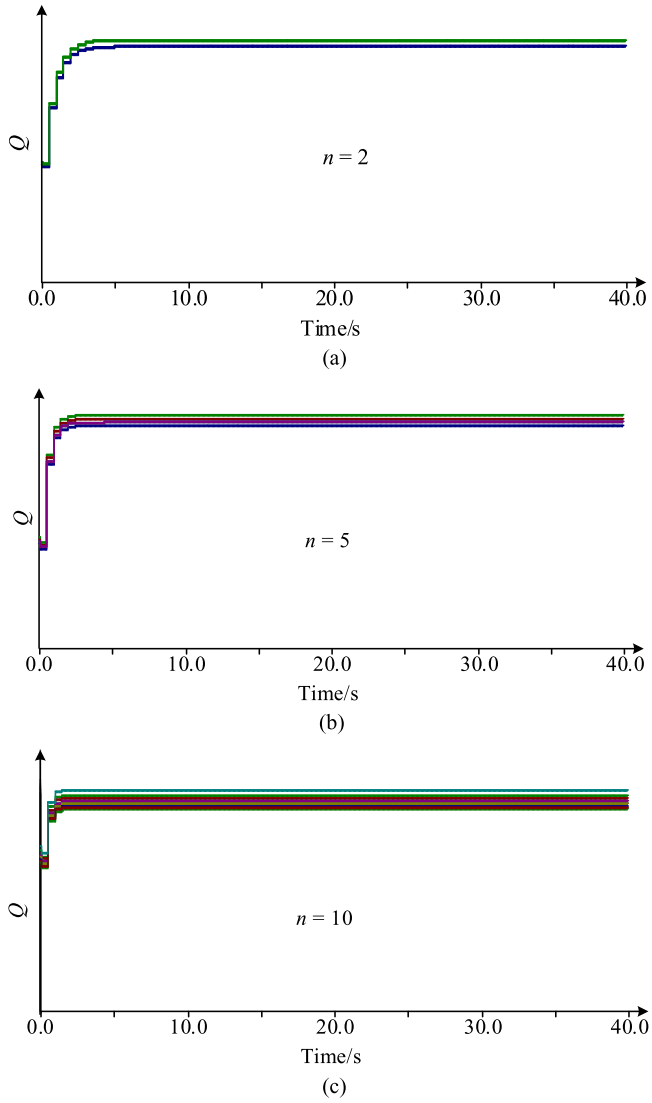

Fig. 8. Simulation results for the DRMSCA with different quantities of DGs: (a) $n = 2$; (b) $n = 5$; (c) $n = 10$.

3) For any quantity of DGs, the proposed DRMSCA can remain stable.

$$\left|\frac{\sum_{i=1}^{n}\frac{k_1-k_i}{(k_i+D_{pi}+\frac{X_i}{E_{ref}})}}{\sum_{i=1}^{n}\frac{k_1+D_{p1}+\frac{X_1}{E_{ref}}}{(k_i+D_{pi}+\frac{X_i}{E_{ref}})}}\right| = \left|\frac{\sum_{i=1}^{n}(k_1-k_i)}{\sum_{i=1}^{n}(k_1+D_{p1}+\frac{X_1}{E_{\mathrm{ref}}})}\right| < 1. \tag{15}$$

To validate the mathematical derivation, two sets of simulations with different communication periods and DG quantities were conducted. The results are shown in Figs. 7 and 8

$$|k_1-k_i| < \left|k_1+D_{p1}+\frac{X_1}{E_{ref}}\right| \tag{16}$$

$$\left|\frac{\sum_{i=1}^{n}\frac{k_1-k_i}{(k_i+D_{pi}+\frac{X_i}{E_{ref}})}}{\sum_{i=1}^{n}\frac{k_1+D_{p1}+\frac{X_1}{E_{ref}}}{(k_i+D_{pi}+\frac{X_i}{E_{ref}})}}\right| = 0 < 1. \tag{17}$$

The communication period is extended in the scenario of $n = 4$, and the DG quantity is increased in the scenario of $T = 0.5$ s.

When the communication period increases continually, the response of the system becomes slower, as shown in Fig. 7(from $T = 0.2$ to 5 s). When the quantity of DGs increases, the response of the system remains stable, as shown in Fig. 8 (from $n = 2$ to 10).

As indicated by the simulation results, when the communication period increases, the system remains stable, even the communication period reaches to 5 s, but with degradation of longer regulation time. Additionally, when the quantity of DGs increases, the system always remains stable. Therefore, the simulation results validate the analysis and conclusions.

C. Effect of Communication Time Delay on Stability of DRMSCA

When there is a communication delay, we can still refer to the foregoing analysis for further research. Here, according to the

communication delay time, three scenarios are considered for analysis.

To simplify the processing, it is considered that the communication delays from the leader to all other units are identical, i.e., τ_{d}.

When $\tau_{\mathrm{d}} < = T$ (*T* represents the communication period):

When a communication period is reached, $t = \mathrm{kT}$ ($k = 0, 1, \ldots$), the reference of the leader is updated, and the second to *n*th DGs remain unchanged. Then, the following can be obtained:

$$\begin{cases} E_{\mathrm{ref}} + k_1 Q_1^{(n)} = (k_1 + D_{p1} + \frac{X_1}{E_{ref}})Q_1 + U_{\mathrm{pcc}} \\ E_{ref} + k_2 Q_1^{(n-1)} = (k_2 + D_{p2} + \frac{X_2}{E_{ref}})Q_2 + U_{pcc} \\ \vdots \\ E_{ref} + k_n Q_1^{(n-1)} = (k_n + D_{pn} + \frac{X_n}{E_{ref}})Q_n + U_{pcc} \\ \sum_{i=1}^{n} Q_i = Q. \end{cases} \tag{18}$$

When the delay time is expired and one communication is complete, i.e., $t = \mathrm{kT} + \tau_{\mathrm{d}}$, the reference of the leader remains unchanged, and the reference of the second to *n*th DGs is updated, then (19) can be obtained. Referring to the mathematical derivation in the previous section, deform and simplify (19) to obtain (20).

Clearly, (20) only represents an intermediate state, and the obtained result can represent the power fluctuation amplitude of the leader caused by communication delay. However, according to (19), it will not affect the system iteration. Referring to the formula (18) in the previous section, it is clear that this formula must converge. Therefore, it can be proven that when the delay time is shorter than the communication period *T*, the system is stable

$$\begin{cases} E_{ref} + k_1 Q_1^{(n)} = (k_1 + D_{p1} + \frac{X_1}{E_{ref}})Q_1 + U_{pcc} \\ E_{ref} + k_2 Q_1^{(n)} = (k_2 + D_{p2} + \frac{X_2}{E_{ref}})Q_2 + U_{pcc} \\ \vdots \\ E_{ref} + k_n Q_1^{(n)} = (k_n + D_{pn} + \frac{X_n}{E_{ref}})Q_n + U_{pcc} \\ \sum_{i=1}^{n} Q_i = Q \end{cases} \tag{19}$$

$$Q_1^{(n+1)} = \frac{Q}{\sum_{i=1}^{n} \frac{k_1 + D_{p1} + \frac{X_1}{E_{ref}}}{k_i + D_{pi} + \frac{X_i}{E_{ref}}}} + \left(\frac{\sum_{i=1}^{n} \frac{k_1}{(k_i + D_{pi} + \frac{X_i}{E_{ref}})} - \sum_{i=1}^{n} \frac{k_i}{(k_i + D_{pi} + \frac{X_i}{E_{ref}})}}{\sum_{i=1}^{n} \frac{k_1 + D_{p1} + \frac{X_1}{E_{ref}}}{(k_i + D_{pi} + \frac{X_i}{E_{\mathrm{ref}}})}} \right) Q_1^{(n)}. \tag{20}$$

When $T < \tau_{\mathrm{d}} < 2T$:

When a communication period is reached, immediately ($k = 0, 1, \ldots$), the reference of the leader is updated, and the second to *n*th DGs remain unchanged, yielding

$$\begin{cases} E_{ref} + k_1 Q_1^{(n)} = (k_1 + D_{p1} + \frac{X_1}{E_{ref}})Q_1 + U_{pcc} \\ E_{ref} + k_2 Q_1^{(n-2)} = (k_2 + D_{p2} + \frac{X_2}{E_{ref}})Q_2 + U_{pcc} \\ \vdots \\ E_{ref} + k_n Q_1^{(n-2)} = (k_n + D_{pn} + \frac{X_n}{E_{ref}})Q_n + U_{pcc} \\ \sum_{i=1}^{n} Q_i = Q \end{cases} \tag{21}$$

$$\begin{cases} E_{ref} + k_1 Q_1^{(n)} = (k_1 + D_{p1} + \frac{X_1}{E_{ref}})Q_1 + U_{pcc} \\ E_{ref} + k_2 Q_1^{(n-1)} = (k_2 + D_{p2} + \frac{X_2}{E_{ref}})Q_2 + U_{pcc} \\ \vdots \\ E_{ref} + k_n Q_1^{(n-1)} = (k_n + D_{pn} + \frac{X_n}{E_{ref}})Q_n + U_{pcc} \\ \sum_{i=1}^{n} Q_i = Q. \end{cases} \tag{22}$$

When the delay time is expired and one communication is complete, i.e., $t = \mathrm{kT} + \tau_{\mathrm{d}}$, the reference of the leader remains unchanged, and the reference of the second to *n*th DGs is updated to the previous reference value, as indicated by (22).

When the communication period is reached for the second time, the reference of the leader is updated again, and the second to *n*th DGs remain unchanged, then the following can be obtained:

$$\begin{cases} E_{ref} + k_1 Q_1^{(n+1)} = (k_1 + D_{p1} + \frac{X_1}{E_{ref}})Q_1 + U_{pcc} \\ E_{ref} + k_2 Q_1^{(n-1)} = (k_2 + D_{p2} + \frac{X_2}{E_{ref}})Q_2 + U_{pcc} \\ \vdots \\ E_{ref} + k_n Q_1^{(n-1)} = (k_n + D_{pn} + \frac{X_n}{E_{ref}})Q_n + U_{pcc} \\ \sum_{i=1}^{n} Q_i = Q. \end{cases} \tag{23}$$

When the delay time τ_{d} is reached again, the reference of the second to *n*th DGs is updated again.

$$\begin{cases} E_{ref} + k_1 Q_1^{(n+1)} = (k_1 + D_{p1} + \frac{X_1}{E_{ref}})Q_1 + U_{pcc} \\ E_{ref} + k_2 Q_1^{(n)} = (k_2 + D_{p2} + \frac{X_2}{E_{ref}})Q_2 + U_{pcc} \\ \vdots \\ E_{ref} + k_n Q_1^{(n)} = (k_n + D_{pn} + \frac{X_n}{E_{ref}})Q_n + U_{pcc} \\ \sum_{i=1}^{n} Q_i = Q. \end{cases} \tag{24}$$

Further deformation and simplification can be performed, as indicated by (25).

There is no doubt that the convergence of (25) indicates that the system has a stable solution, that is, the system can be finally stable. However, whether (25) converges mainly depends on the coefficients of $Q1^{(n)}$ and $Q1^{(n-1)}$; here, *a* and *b* are the iteration coefficients. Because the iterative format contains the former two steps of iterative information, the actual iterative forward sweep is complex. When the values of *a* and *b* change, the system has countless possibilities. To draw meaningful conclusions and promote the practical application of the proposed method, we

refer to the assumptions presented in the previous section

$$Q_1^{(n+1)} = \frac{Q}{\sum_{i=1}^{n} \frac{k_1+D_{p1}+\frac{X_1}{E_{ref}}}{k_i+D_{pi}+\frac{X_i}{E_{ref}}}} - \left(\frac{\frac{k_1}{(k_1+D_{p1}+\frac{X_1}{E_{ref}})} - \sum_{i=1}^{n} \frac{k_i}{(k_i+D_{pi}+\frac{X_i}{E_{ref}})}}{\sum_{i=1}^{n} \frac{k_1+D_{p1}+\frac{X_1}{E_{ref}}}{(k_i+D_{pi}+\frac{X_i}{E_{ref}})}} \right) Q_1^{(n)} - \left(\frac{\sum_{i=2}^{n} \frac{k_i}{(k_i+D_{pi}+\frac{X_i}{E_{ref}})}}{\sum_{i=1}^{n} \frac{k_1+D_{p1}+\frac{X_1}{E_{ref}}}{(k_i+D_{pi}+\frac{X_i}{E_{ref}})}} \right) Q_1^{(n-1)} \tag{25}$$

$$k_1 = k_2 = \cdots = k_n = k. \tag{26}$$

Thus, (27) and (28) can be easily obtained:

$$-1 < \frac{\frac{k_1}{(k_1+D_{p1}+\frac{X_1}{E_{ref}})} - \sum_{i=1}^{n} \frac{k_i}{(k_i+D_{pi}+\frac{X_i}{E_{ref}})}}{\sum_{i=1}^{n} \frac{k_1+D_{p1}+\frac{X_1}{E_{ref}}}{(k_i+D_{pi}+\frac{X_i}{E_{ref}})}} < 0. \tag{27}$$

Considering conditions (27) and (28), we can derive the only solution (25) that will converge, and the system converges.

When $2T < \tau_{\mathrm{d}}$ (T represents the communication period), an expression similar to (23) can be derived. However, the iterative expression has more terms, and each term is multiplied by a coefficient. With a longer delay, there will be more terms, and the expression will be more complex. It can be difficult to determine whether the solution converges and thus impossible to judge the stability of the system. However, we have drawn a relatively conservative conclusion; that is, when the communication delay is shorter than $2T$, the system must remain stable. Recall the previous conclusion that the communication period does not affect the stability of the system. Therefore, when the communication delay is long, there can be a theoretical basis to alleviate the contradiction by increasing the communication period.

In summary, when there is a communication delay, the conservative delay stability limit can be obtained as $\tau_{\mathrm{d}} < 2T$. When the delay is longer than $2T$, the system may be stable or unstable, and no clear conclusion can be drawn. However, the analysis presented in the previous section indicated that the communication period of the DRMSCA can generally be adjusted according to requirements and has little effect on the system stability. Therefore, when there is a long communication delay, the communication period can be extended, which can significantly improve the communication delay tolerance

$$0 < \frac{\sum_{i=2}^{n} \frac{k_i}{(k_i+D_{pi}+\frac{X_i}{E_{ref}})}}{\sum_{i=1}^{n} \frac{k_1+D_{p1}+\frac{X_1}{E_{ref}}}{(k_i+D_{pi}+\frac{X_i}{E_{ref}})}} < 1. \tag{28}$$

To verify the correctness of the analysis, simulations involving the communication delay were conducted. As shown in Fig. 9, even when the communication delay is increased to twice the communication period, i.e., approximately 10 s, the system can remain stable. Therefore, the simulation results validate the analysis.

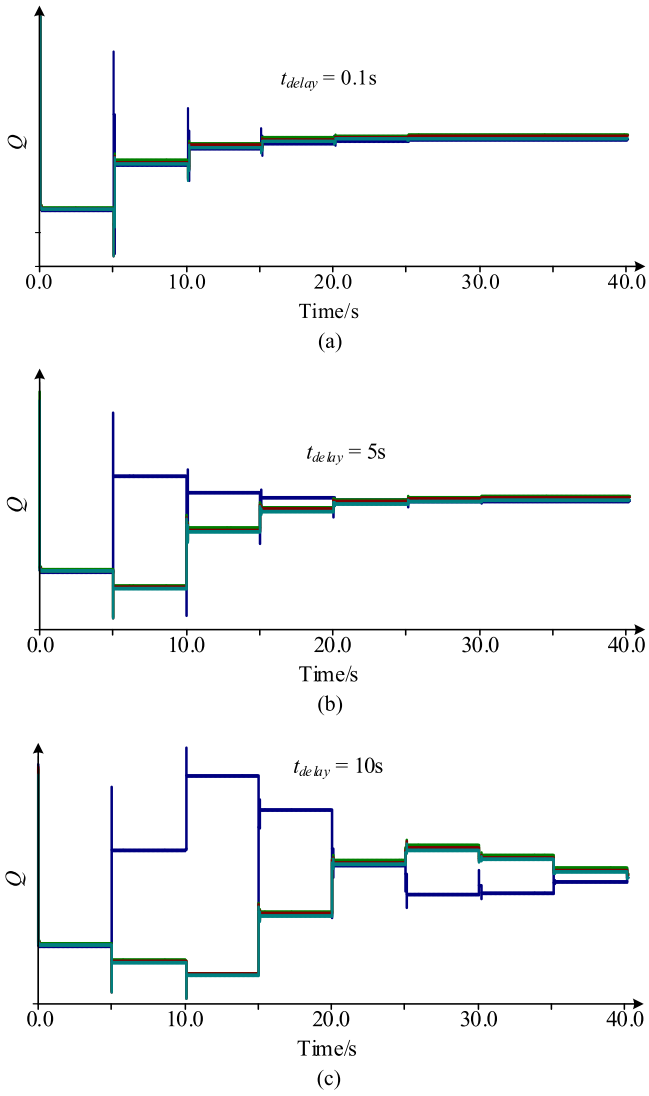

Fig. 9. Simulation results for the DRMSCA with different communication delays: (a) $t_{\mathrm{delay}} = 0.1$ s; (b) $t_{\mathrm{delay}} = 5$ s; (c) $t_{\mathrm{delay}} = 10$ s.

D. Parameter Selection of DRMSCA

The key parameters of the DRMSCA include the proportional coefficient k_{qv} of the outer loop and the PI parameters k_p and k_i of the inner loop. The basic principles of their selection include two aspects as follows:

1) ensure the stability of the local controller;
2) ensure the stability of the MG system;
3) ensure that the steady-state error of power sharing is reduced to the greatest extent possible.

For the stability of the local controller, the acceptable range of k_{qv}, k_p, and k_i can be determined by establishing the local controller small signal model. For detailed methods, please refer to the author's previous work [33].

To ensure the stability of the system—particularly in cases of a long communication delay—(27) and (28) must be satisfied.

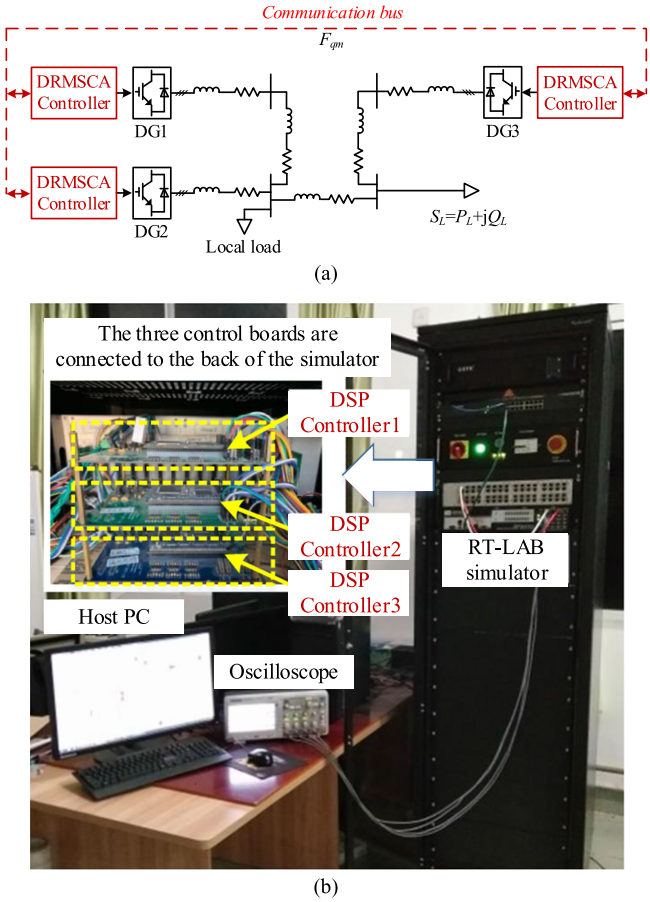

Fig. 10. HIL experimental platform: (a) experimental circuit and (b) HIL platform.

Because the selection of k in the DRMSCA has weak correlations with local information such as the capacity and voltage of the micro-sources, it is easy to set the k values of all the micro-sources to be equal, so that (27) and (28) are always satisfied, ensuring the stability of the system when the communication cycle is relatively long and there is a long communication delay within $2T$.

To ensure that the steady-state error of power sharing is as small as possible, k_{qv} should be as large as possible, on the premise of ensuring the system stability.

Using the three foregoing conditions, appropriate DRMSCA control parameters can be selected.

IV. Experimental Verification

The experimental verification mainly included the verification of the basic functions, power-sharing performance in multiple operating scenarios (voltage regulation, load fluctuation, communication delay and fault, DG fault and clearance), voltage recovery, communication delay, and failure.

To verify the feasibility of the proposed method, a control hardware in the loop test platform of the island MG was established, as shown in Fig. 10.

The main circuit part of the system was simulated using the RT-LAB real-time simulator, the control part was implemented using three DSP controllers (TMS320F28335), the communication part was implemented using a CAN bus, the communication line was a copper core shielded twisted pair, and the communication speed was set as 10 kbps. The difference delay coefficient was $k = 0.025$, with $T_{\mathrm{seen}} = 0.2$ s. The rated frequency of the MG was 50 Hz, the rated single-phase voltage was 220 V, the rated active power was 23 kW, and the rated reactive power was 13 kVar.

TABLE I
VSG Parameters

Parameter	VSG_1	VSG_2	VSG_3
J	0.5066	0.8106	1.0132
K	6283.185	9424.778	15707.963
D_p	5.066	8.106	10.132
D_q	200	300	500
P_n(kW)	5	8	10
Q_n(kVar)	4	4	5
f_n(Hz)	50	50	50
V_n(V)	220	220	220

TABLE II
DRMSCA Parameters of VSGs

Parameter	VSG_1	VSG_2	VSG_3
k_{qv}	28	30	30
k_p	10	15	20
k_i	500	300	200

A. System Parameters

When the proposed method is adopted, the missing power caused by the failure of the VSG can be automatically shared with other DGs according to the capacity ratio. To verify this advantage, three VSGs were used in the experiment to construct an MG platform. Tables I and II present the VSG parameters and the new link part PI parameters. The VSG switching frequency was 6.4 kHz, the output filter $L = 3$ mH, $C = 6$ μF. The power calculation low-pass filter parameters were $G_1 = 1$ and $T_1 = 0.02$ in the DSP program [33], [38]–[40].

To fully verify the performance of the proposed method, three experimental settings were applied, as explained in the following subsection.

B. Voltage Regulation Experiment Results

The main objective of this group of experiments was to verify the voltage fluctuation function of the proposed method with power fluctuation. The process was as follows. In the initial stage, the VSG MG had a light load of 12 kW and 5 kVar. At 50 s, the active load of 10 kVar was input. The reactive load became 15 kVar. At 65 s, the DRMSCA was put into operation. At 80 s, the reactive load of 10 kVar was removed, and the total reactive load became 5 kVar. At 95 s, the active load of 10 kVar was reapplied, and the total active load became 15 kVar. At 110 s, VSG1 was disconnected because of a fault.

Fig. 11(a) presents the regulation of the system voltage under the fluctuations of different loads. As shown, in the first stage (<50 s), the DRMSCA was not put into operation. At this

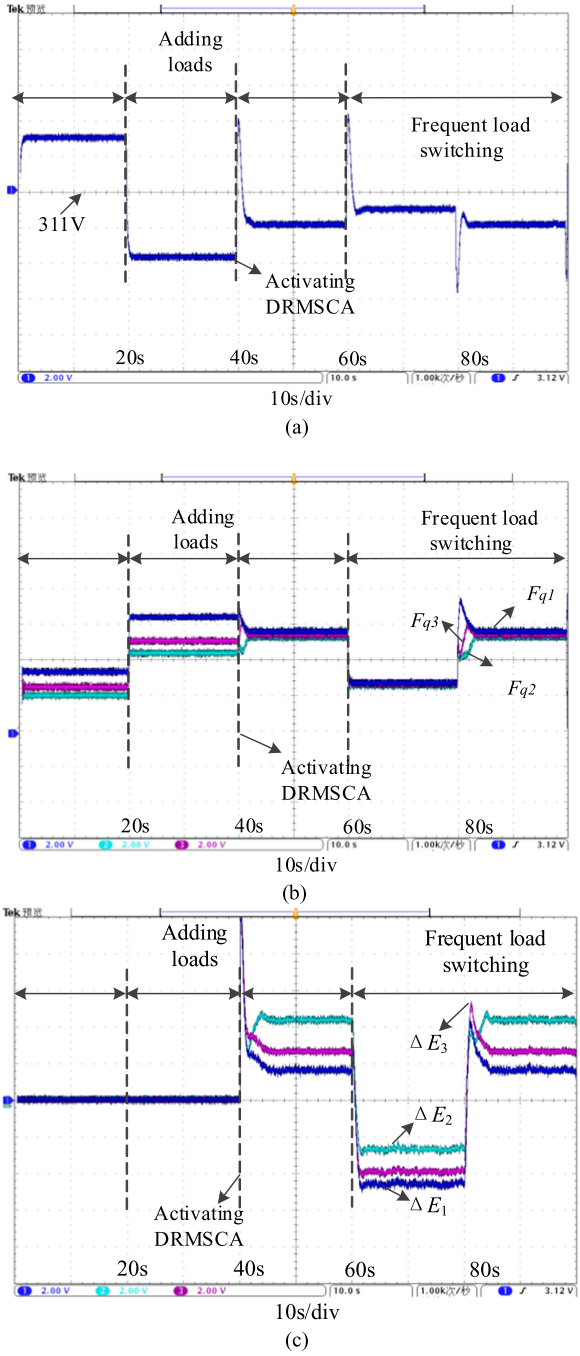

Fig. 11. DRMSCA performance test waveforms: (a) voltage recovery characteristics; (b) output factor; (c) voltage reference regulation. Blue, green, and purple correspond to VSG1, VSG2, and VSG3, respectively.

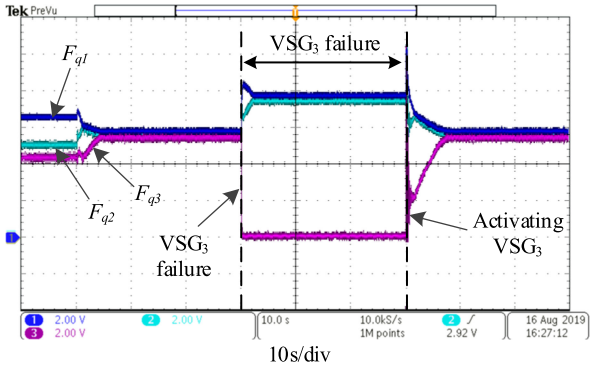

Fig. 12. Performance test waveforms for the VSG_3 fault resection. Blue, green, and purple correspond to VSG_1, VSG_2, and VSG_3, respectively.

time, the system was lightly loaded. Because of the drooping characteristics of the VSG, the PCC voltage was stable at approximately 314.5 V, which was slightly higher than the rated voltage. In the second stage (50–65 s), the system load increased to 6 kVar, which exceeded the rated power of the system. The system voltage decreased to approximately 307.2 V, which was slightly lower than the rated voltage. In the third stage (>65 s), the DRMSCA started at 65 s. At this time, the system operating voltage was lower than the rated value. The voltage inner loop of the DRMSCA in each VSG outputted the voltage given compensation amount and adjusted the reactive output of the inverter, and finally the voltage of the system recovered to near 311 V. Then, when 80 s 18 kW load shedding, 95 s 18 kW load input and 110 s VSG1 exit operation, the regulation process is similar. Clearly, the DRMSCA can achieve secondary voltage control performance when the system load fluctuates.

Fig. 11(b) presents a waveform diagram of the output factor, which reflects the distribution of the output for the three VSGs. As shown, from 0 to 65 s, the DRMSCA was not put into operation. At this time, although the VSGs of the system had droop characteristics, the output factors of the VSGs were not equal, owing to the influence of the line impedance. Because the DRMSCA was not put into use in this stage, the output compensation amount, i.e., the voltage reference given regulation amount, was always 0. At 65 s, the DRMSCA was put into operation, which affected the power allocation in the steady state of the system, and each VSG could achieve the power ratio according to the principle of equal output factors.

Fig. 11(c) presents the voltage reference regulation amount for the three VSGs. As shown, when the DRMSCA was put into operation, the voltage setting of the VSG could be regulated (the regulation value was approximately 5:8:10), and the proportional distribution of the output power of each VSG was achieved. Furthermore, as shown in Fig. 12, after 110 s, even if VSG3 was out of operation, the load power could be redistributed according to the rated-power ratio of VSG2 to VSG3. At 140 s, VSG3 was put back into operation, three VSGs could still be restored to the state of power sharing.

According to the foregoing analysis, the proposed method achieved voltage control and reactive power sharing when the load fluctuated.

C. *Effects of Communication Delay and Failure*

The main objectives of this group of experiments were to verify the impact of the low-bandwidth performance of the proposed method on the system reliability and to compare it with the traditional consistency [34]. The communication delay of VSG1 was set as 0.2 and 1 s, and the communication was completely invalid, and the comparison was demonstrated. The change process of the system was as follows. In the initial stage,

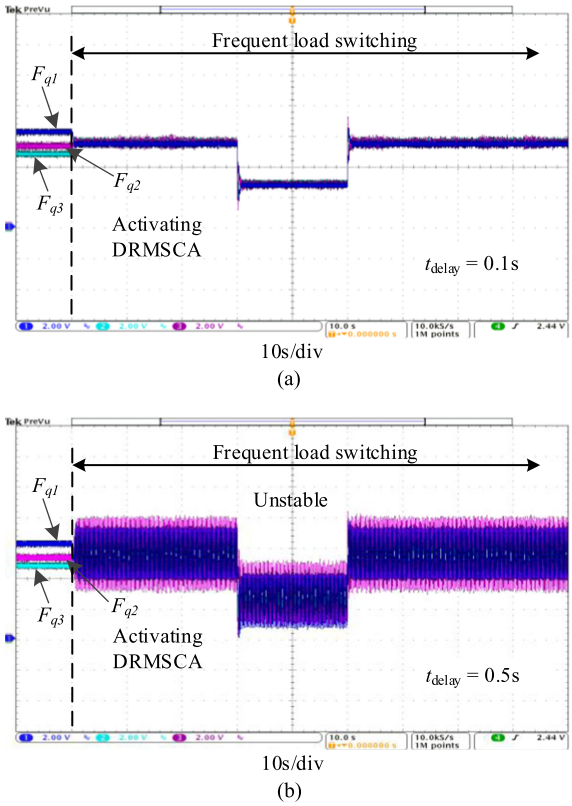

Fig. 13. Conventional consensus-based secondary control for communication latency of 0.1 s and 0.5 s in VSG_1, respectively; VSG_1 (blue), VSG_2 (green), VSG_3 (purple).

the VSG-based MG had a light load of 12 kW and 5 kVar. At 50 s, an active load of 18 kW was input; thus, the total active power became 30 kW. At 65 s, the DRMSCA was put into operation.

According to Fig. 13, when the proposed method is used, even if the communication period is 0.1, 0.5, or 1 s, the system can achieve voltage recovery and equalization of the reactive power under load fluctuations. As the communication period increases, the regulation performance of the system voltage and the power distribution accuracy remain almost unchanged, but the response time of the power distribution increases. There are two main reasons for this. First, the voltage regulation function of the proposed method is independently completed by the control systems of the DGs. Second, the communication system only transmits a unified reference signal to each unit to coordinate the DGs. When the communication period is long, the number of times that other units simultaneously receive valid information becomes small, which reduces the number of regulations of other units, resulting in a slower response of the outer-loop power sharing.

Additionally, we compared the proposed DRMSCA with the conventional consensus-based control method [29], as shown in Figs. 13 and 14. When the communication delay was 0.1 s, both methods remained stable. However, when the communication delay reached 0.5 s, the traditional method became unstable, and the system oscillated. The proposed method remained stable even when the communication delay reached 1 s, confirming its advantages.

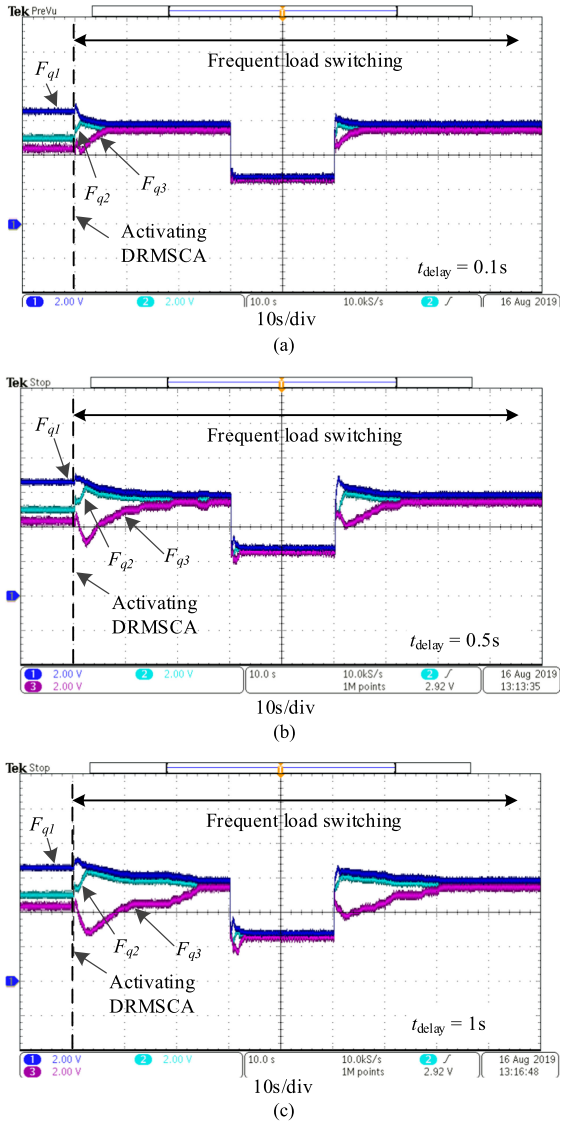

Fig. 14. Performance of DRMSCA for communication latency of 0.1, 0.5, and 1 s in VSG_1, respectively; VSG_1 (blue), VSG_2 (green), VSG_3 (purple).

Therefore, even if there is a delay in communication, it will only affect the response speed of the system power proportionally. It will not affect the accuracy or speed of the controllers' voltage regulation. The system can still operate reliably.

According to the foregoing analysis, this set of experiments verified the advantages of low-bandwidth communication methods and their effects on the system voltage recovery and distribution reliability.

V. Conclusion

To overcome the trade-off between voltage control and reactive power sharing in islanded MGs, a dynamical reconfigurable master–slave control strategy is proposed in this article. The following conclusions are drawn.

1) DRMSCA can control the voltage fluctuation of island MGs under a low communication bandwidth more effectively than existing methods.

2) The quantity of DGs and communication period have little effect on the DRMSCA; even if the communication period is around the "*s*" level or above, the proposed DRMSCA can operate normally.
3) The DRMSCA is hardly affected by communication delays, and when the communication delay is shorter than $2T$, the system remains stable.
4) When the communication fails, the DRMSCA can always ensure that there is only one leader in the MG. Thus, there is no brain splitting caused by communication failure, and the system is safe and reliable.

ACKNOWLEDGMENT

The authors would like to thank Zhen Tian, Yuexi Tang, and Daming Wang for their valuable suggestion and help, which have considerably improved the quality of this article.

REFERENCES

[1] J. Rocabert, A. Luna, F. Blaabjerg, and P. Rodríguez, "Control of power converters in AC microgrids," *IEEE Trans. Power Electron.*, vol. 27, no. 11, pp. 4734–4749, Nov. 2012.
[2] J. M. Guerrero, J. C. Vasquez, J. Matas, L. G. de Vicuna, and M. Castilla, "Hierarchical control of droop-controlled AC and DC microgrids—A general approach toward standardization," *IEEE Trans. Ind. Electron.*, vol. 58, no. 1, pp. 158–172, Jan. 2011.
[3] A. L. Dimeas and N. D. Hatziargyriou, "Operation of a multiagent system for microgrid control," *IEEE Trans. Power Syst.*, vol. 20, no. 3, pp. 1447–1455, Aug. 2005.
[4] H. Jiayi, J. Chuanwen, and X. Rong, "A review on distributed energy resources and microgrid," *Renewable Sustain. Energy Rev.*, vol. 12, no. 9, pp. 2472–2483, Dec. 2008.
[5] Q. Zhou, M. Shahidehpour, A. Paaso, S. Bahramirad, A. Alabdulwahab, and A. Abusorrah, "Distributed control and communication strategies in networked microgrids," *IEEE Commun. Surv. Tut.*, vol. 22, no. 4, pp. 2586–2633, Oct.–Dec. 2020.
[6] Z. Shuai, W. Huang, Z. J. Shen, A. Luo, and Z. Tian, "Active power oscillation and suppression techniques between two parallel synchronverters during load fluctuations," *IEEE Trans. Power Electron.*, vol. 35, no. 4, pp. 4127–4142, Apr. 2020.
[7] Q. Mei, M. Shan, L. Liu, and J. M. Guerrero, "A novel improved variable step-size incremental-resistance MPPT method for PV systems," *IEEE Trans. Ind. Electron.*, vol. 58, no. 6, pp. 2427–2434, Jun. 2011.
[8] Z. Shuai *et al.*, "Microgrid stability: Classification and a review," *Renewable Sustain. Energy Rev.*, vol. 58, pp. 167–179, May 2016.
[9] H. Han, X. Hou, J. Yang, J. Wu, M. Su, and J. M. Guerrero, "Review of power sharing control strategies for islanding operation of AC microgrids," *IEEE Trans. Smart Grid*, vol. 7, no. 1, pp. 200–215, Jan. 2016.
[10] Y. W. Li and C. Kao, "An accurate power control strategy for power-electronics-interfaced distributed generation units operating in a low-voltage multibus microgrid," *IEEE Trans. Power Electron.*, vol. 24, no. 12, pp. 2977–2988, Dec. 2009.
[11] Q. Zhong and G. Weiss, "Synchronverters: Inverters that mimic synchronous generators," *IEEE Trans. Ind. Electron.*, vol. 58, no. 4, pp. 1259–1267, Apr. 2011.
[12] P. Piagi and R. H. Lasseter, "Autonomous control of microgrids," in *Proc. IEEE Power Eng. Soc. General Meeting*, 2006, p. 8. [Online]. Available: http://ieeexplore.ieee.org/stamp/stamp.jsp?tp=&arnumber=1708993
[13] M. C. Chandorkar, D. M. Divan, and R. Adapa, "Control of parallel connected inverters in standalone AC supply systems," *IEEE Trans. Ind. Appl.*, vol. 29, no. 1, pp. 136–143, Jan./Feb. 1993.
[14] J. M. Guerrero, L. G. I. A. De Vicu N A, J. E. Matas, M. Castilla, and J. Miret, "Output impedance design of parallel-connected UPS inverters with wireless load-sharing control," *IEEE Trans. Ind. Electron.*, vol. 52, no. 4, pp. 1126–1135, Aug. 2005.
[15] J. M. Guerrero, M. Chandorkar, T. Lee, and P. C. Loh, "Advanced control architectures for intelligent microgrids—Part I: Decentralized and hierarchical control," *IEEE Trans. Ind. Electron.*, vol. 60, no. 4, pp. 1254–1262, Apr. 2012.
[16] J. He, Y. W. Li, J. M. Guerrero, F. Blaabjerg, and J. C. Vasquez, "An islanding microgrid power sharing approach using enhanced virtual impedance control scheme," *IEEE Trans. Power Electron.*, vol. 28, no. 11, pp. 5272–5282, Nov. 2013.
[17] C. T. Lee, C. C. Chuang, and C. C. Chu, "Control strategies for distributed energy resources interface converters in the low voltage microgrid," in *Proc. IEEE Energy Convers. Congr. Expo.*, 2009, pp. 2022–2029.
[18] Q. Zhong, "Robust droop controller for accurate proportional load sharing among inverters operated in parallel," *IEEE Trans. Ind. Electron.*, vol. 60, no. 4, pp. 1281–1290, Apr. 2013.
[19] J. M. Rey, P. Martí, M. Velasco, J. Miret, and M. Castilla, "Secondary switched control with no communications for islanded microgrids," *IEEE Trans. Ind. Electron.*, vol. 64, no. 11, pp. 8534–8545, Nov. 2017.
[20] J. A. P. Lopes, C. L. Moreira, and A. G. Madureira, "Defining control strategies for microgrids islanded operation," *IEEE Trans. Power Syst.*, vol. 21, no. 2, pp. 916–924, May 2006.
[21] Q. Shafiee, J. M. Guerrero, and J. C. Vasquez, "Distributed secondary control for islanded microgrids—A novel approach," *IEEE Trans. Power Electron.*, vol. 29, no. 2, pp. 1018–1031, Feb. 2014.
[22] J. W. Simpson-Porco, F. D O Rfler, and F. Bullo, "Synchronization and power sharing for droop-controlled inverters in islanded microgrids," *Automatica*, vol. 49, no. 9, pp. 2603–2611, Sep. 2013.
[23] O. Mégel, T. Liu, D. J. Hill, and G. Andersson, "Distributed secondary frequency control algorithm considering storage efficiency," *IEEE Trans. Smart Grid*, vol. 9, no. 6, pp. 6214–6228, Nov. 2018.
[24] A. Bidram, A. Davoudi, F. L. Lewis, and J. M. Guerrero, "Distributed cooperative secondary control of microgrids using feedback linearization," *IEEE Trans. Power Syst.*, vol. 28, no. 3, pp. 3462–3470, Aug. 2013.
[25] F. Guo, C. Wen, J. Mao, and Y. Song, "Distributed secondary voltage and frequency restoration control of droop-controlled inverter-based microgrids," *IEEE Trans. Ind. Electron.*, vol. 62, no. 7, pp. 4355–4364, Jul. 2015.
[26] L. Lu and C. Chu, "Consensus-based droop control synthesis for multiple DICs in isolated micro-grids," *IEEE Trans. Power Syst.*, vol. 30, no. 5, pp. 2243–2256, Sep. 2015.
[27] J. W. Simpson-Porco, Q. Shafiee, F. Dörfler, J. C. Vasquez, J. M. Guerrero, and F. Bullo, "Secondary frequency and voltage control of islanded microgrids via distributed averaging," *IEEE Trans. Ind. Electron.*, vol. 62, no. 11, pp. 7025–7038, Nov. 2015.
[28] Q. Zhou, Z. Tian, M. Shahidehpour, X. Liu, A. Alabdulwahab, and A. Abusorrah, "Optimal consensus-based distributed control strategy for coordinated operation of networked microgrids," *IEEE Trans. Power Syst.*, vol. 35, no. 3, pp. 2452–2462, May 2020.
[29] J. Zhou, S. Kim, H. Zhang, Q. Sun, and R. Han, "Consensus-based distributed control for accurate reactive, harmonic, and imbalance power sharing in microgrids," *IEEE Trans. Smart Grid*, vol. 9, no. 4, pp. 2453–2467, Jul. 2018.
[30] M. S. Golsorkhi, D. J. Hill, and M. Baharizadeh, "A secondary control method for voltage unbalance compensation and accurate load sharing in networked microgrids," *IEEE Trans. Smart Grid*, vol. 12, no. 4, pp. 2822–2833, Jul. 2021.
[31] L. Xing, F. Guo, X. Liu, C. Wen, Y. Mishra, and Y. C. Tian, "Voltage restoration and adjustable current sharing for DC microgrid with time delay via distributed secondary control," *IEEE Trans. Sustain. Energy*, vol. 12, no. 2, pp. 1068–1077, Apr. 2021.
[32] R. W. Erickson and D. Maksimovic, *Fundamentals of Power Electronics*. Berlin, Germany: Springer Science & Business Media, 2007.
[33] Z. Shuai, W. Huang, X. Shen, Y. Li, X. Zhang, and Z. J. Shen, "A maximum power loading factor (MPLF) control strategy for distributed secondary frequency regulation of islanded microgrid," *IEEE Trans. Power Electron.*, vol. 34, no. 3, pp. 2275–2291, Mar. 2019.
[34] R. Olfati-Saber and R. M. Murray, "Consensus problems in networks of agents with switching topology and time-delays," *IEEE Trans. Autom. Control*, vol. 49, no. 9, pp. 1520–1533, Sep. 2004.
[35] L. Meng *et al.*, "Distributed voltage unbalance compensation in islanded microgrids by using a dynamic consensus algorithm," *IEEE Trans. Power Electron.*, vol. 31, no. 1, pp. 827–838, Jan. 2016.
[36] X. Lu, X. Yu, J. Lai, J. M. Guerrero, and H. Zhou, "Distributed secondary voltage and frequency control for islanded microgrids with uncertain communication links," *IEEE Trans. Ind. Inform.*, vol. 13, no. 2, pp. 448–460, Apr. 2017.
[37] R. Olfati-Saber, J. A. Fax, and R. M. Murray, "Consensus and cooperation in networked multi-agent systems," in *Proc. IEEE*, vol. 97, no. 1, pp. 215–233, Jan. 2007.

[38] K. Yu, Q. Ai, S. Wang, J. Ni, and T. Lv, "Analysis and optimization of droop controller for microgrid system based on small-signal dynamic model," *IEEE Trans. Smart Grid*, vol. 7, no. 2, pp. 695–705, Mar. 2016.
[39] W. Yao, M. Chen, J. E. Matas, J. M. Guerrero, and Z. Qian, "Design and analysis of the droop control method for parallel inverters considering the impact of the complex impedance on the power sharing," *IEEE Trans. Ind. Electron.*, vol. 58, no. 2, pp. 576–588, Feb. 2011.
[40] S. Ullah, L. Khan, I. Sami, and N. Ullah, "Consensus-Based delay-tolerant distributed secondary control strategy for droop controlled AC microgrids," *IEEE Access*, vol. 9, pp. 6033–6049, 2021.

Wen Huang (Member, IEEE) received the B.S. and Ph.D. degrees in electrical engineering from Hunan University, Changsha, China, in 2014 and 2020 respectively.

During 2018–2020, he was a Visiting Scholar with the Department of Electrical and Computer Engineering, Illinois Institute of Technology, Chicago, IL, USA. He is currently a Postdoctoral Researcher with the College of Electrical and Information Engineering, Hunan University. His research interests include renewable energy, fault analysis, and control of converters.

Zhikang Shuai (Senior Member, IEEE) received the B.S. and Ph.D. degrees in electrical engineering from the College of Electrical and Information Engineering, Hunan University, Changsha, China, in 2005 and 2011, respectively.

He was with Hunan University, as an Assistant Professor between 2009 and 2012, an Associate Professor in 2013, and a Professor in 2014. His research interests include power quality control, power electronics, and microgrid stability analysis and control.

Prof. Shuai is the Associate Editor of the *CSEE Journal of Power and Energy Systems* and the *Chinese Journal of Electrical Engineering*. He was the recipient of the 2010 National Scientific and Technological Awards of China, the 2012 Hunan Technological Invention Awards of China, and the 2007 Scientific and Technological Awards from the National Mechanical Industry Association of China.

Xia Shen received the B.S. degree in electrical engineering from Jiangsu University, Zhenjiang, China, in 2016. She is currently working toward the Ph.D. degree in power electronics with the College of Electrical Engineering, Hunan University, Changsha, China.

Her research interests include hybrid microgrid, fault analysis, and synchronization control of converters.

Yifeng Li received the B.S. and M.S. degrees in electrical engineering from Hunan University, Changsha, China, in 2017 and 2020, respectively.

He is currently with the State Grid Corporation of China, Changsha, China. His research interests include renewable energy and control of converters in microgrids.

Z. John Shen (Fellow, IEEE) received the B.S. degree from Tsinghua University, Beijing, China, in 1987, and the M.S. and Ph.D. degrees from Rensselaer Polytechnic Institute, Troy, NY, USA, in 1991 and 1994, respectively, all in electrical engineering.

He was a Faculty with the University of Michigan-Dearborn, Dearborn, MI, USA, between 1999 and 2004, and with the University of Central Florida, Orlando, FL, USA, between 2004 and 2012. He joined the Illinois Institute of Technology, Chicago, IL, USA, in 2013, as the Grainger Chair Professor in Electrical and Power Engineering. He has also held a courtesy professorship with Hunan University, Changsha, China, since 2007; and with Zhejiang University, Hangzhou, China, since 2013. His research interests include power electronics and power semiconductor devices.

Dr. Shen has been an active volunteer in the IEEE Power Electronics Society, and has served as a VP of Products from 2009 to 2012, Associate Editor and Guest Editor-in-Chief of the IEEE TRANSACTIONS ON POWER ELECTRONICS, technical program chair and general chair of several major IEEE conferences.